LONG-TERM PERFORMANCE OF ALUMINIDE COATINGS ON Fe-BASE ALLOYS

Bruce A. Pint
Oak Ridge National Laboratory, P.O. Box 2008, Oak Ridge, TN 37831-6156
E-mail: pintba@ornl.gov; Telephone: (865) 576-2897; Fax: (865) 241-0215

Ying Zhang
Department of Mechanical Engineering, Tennessee Technological University, P.O.Box 5014, Cookeville, TN 38505-0001
E-mail: yzhang@tntech.edu; Telephone: (931) 372-3265; Fax: (931) 372-6340

Sebastien Dryepondt
Oak Ridge National Laboratory, P.O. Box 2008, Oak Ridge, TN 37831-6156
E-mail: dryepondtsn@ornl.gov; Telephone: (865) 576-2894; Fax: (865) 241-0215

L. R. Walker
Oak Ridge National Laboratory, P.O. Box 2008, Oak Ridge, TN 37831-6064
E-mail: walkerlr@ornl.gov; Telephone: (865) 574-5339; Fax: (865) 576-5413

Ian G. Wright
Oak Ridge National Laboratory, P.O. Box 2008, Oak Ridge, TN 37831-6156
E-mail: wrightig@ornl.gov; Telephone: (865) 574-4451; Fax: (865) 241-0215

ABSTRACT

Aluminide coatings made by chemical vapor deposition on representative ferritic (Fe-9Cr-1Mo) and austenitic (Type 304L) substrates were evaluated after exposure in humid air at 650°-800°C. A humid air environment was used to identify coating failure during exposure, as uncoated substrates experience rapid oxidation at these temperatures. One goal of this work was to demonstrate the potential benefits and problems with alumina-forming coatings. The higher exposure temperatures were selected to accelerate the degradation of the coating by interdiffusion with the substrate. These results support development of a coating lifetime model. The critical Al content of the coating at which failure occurs is a key parameter needed to complete the model, and a coating failure after ~10kh at 700°C provides some information. Another goal of the work was to examine the effect of the coating on the substrate creep properties. Creep rates are reported at 650°C with and without coatings and with various heat treatments.

INTRODUCTION

Enriching the surface of high-performance alloys with Al to improve their environmental resistance by forming a protective external alumina scale has been studied for many years.[1-12] Alumina-forming coatings are used at higher temperatures (>900°C), where the slow growth rate of an alumina scale and its stability in the presence of water vapor[13] are superior to coatings that form chromia or silica-rich scales. Chromia-forming coatings are more widely employed at lower temperatures for Fe-base alloys in environments such as steam. However, with a goal of ultra-supercritical (USC) steam coal-fired power plants,[14] the higher temperatures will increase the H_2O-accelerated volatility of chromia and silica scales[13] and require more stable alumina scales formed by Al-rich coatings.

For USC-type applications, several research groups are developing aluminide coatings compatible with the heat treatment schedule of ferritic-martensitic steels (e.g. Fe-9Cr)[10,11] and on methods for coating large

components such as weld-overlay.[15] Another objective is to clearly define the inherent benefits and problems with aluminide coatings on Fe-base ferritic (e.g. Fe-9Cr-1Mo, T91) and austenitic (e.g. Fe-18Cr-8Ni, 304L) substrates to justify their usage and improve their durability.[16-19] An aluminide coating lifetime model is being developed, based on long-term interdiffusion studies.[16] One long-term performance problem with aluminide coatings may be associated with degradation due to the coefficient of thermal expansion (CTE) mismatch between aluminides and these substrates[17,18] and the loss of strength due to the interdiffusion of Al into the substrate.[19] As part of this work, long-term oxidation studies were conducted at 650°-800°C on model aluminide coatings made in a controlled, laboratory-scale chemical vapor deposition (CVD) process.[20] An environment of air + 10vol.% water vapor was used as a low cost (compared to steam) method for determining coating performance. Unlike dry air, many Fe-base alloys are rapidly oxidized in wet air when not coated,[17,18,21] thereby providing an indication when the coating is no longer effective. One of the limitations of the lifetime model[16] has been estimating the critical Al content for coating failure, C_b. Some information was available from Fe-Al-Cr alloys[22,23] but a recent coating failure at 700°C has provided a more relevant indication of C_b. A summary of the first series of creep experiments also is included with recommendations for future work.

EXPERIMENTAL PROCEDURE

Substrates (~1.5mm thick) coated were commercial T91 (Fe-9.3at.%Cr-0.56Mo-0.46Mn-0.26V-0.55Si-0.15Ni-0.46C-0.22N-0.005S), P92 (Fe-9.9at.%Cr-0.55%W-0.30Mo-0.46Mn-0.26V-0.32Si-0.12Ni-0.51C-0.23N-0.009S) and commercial type 304L stainless steel (Fe-19.7at%Cr-7.9Ni-1.81Mn-0.15Mo-0.76Si-0.32N-0.09C-0.006S). The laboratory-scale CVD reactor and coating process for low-activity (thin coatings formed after 6h at 900°C with ~5μm Al-rich outer layer and ~50μm total thickness including the interdiffusion zone) and high-activity (thick coatings formed after 4h at 1050°C with ~20-40μm outer layer and ~150-275μm total thickness on T91) as well as the as-coated microstructure are described elsewhere.[16-18,24] (Typical as-deposited Al profiles for these coatings are shown in Figures 4 and 9.) For comparison, similar coatings were made by a laboratory-scale pack cementation process[25] which is more relevant to commercial coating processes. Coated specimens were exposed with the as-coated surface finish and were cleaned in acetone and methanol prior to exposure. Mass changes (±0.01mg/cm²) were measured using a Mettler Toledo model AG245 balance. Cyclic oxidation exposures were conducted with a 100h cycle time with specimens in an alumina boat with faces parallel to the gas stream. Distilled water was atomized into the flowing gas stream (850ml/min) through an alumina tube (e.g. gas velocity of 1.7cm/s at 700°C) and was calibrated to 10±1 vol.% based on the amount of water injected. Creep tests were performed at 650°C in laboratory air on 25mm long dog bone specimens with a gage section of 2 x 2mm, a 600grit finish and loads of 100-140MPa. The load was calculated based on the entire gage including any applied coating and selected to lead to rupture in <1kh. Corrosion and creep specimens were examined by field emission gun, scanning electron microscopy (SEM) equipped with energy dispersive x-ray analysis (EDXA), and by electron probe microanalysis (EPMA) using wavelength dispersive x-ray analysis. Coated specimens were examined in plan view every 2kh by SEM. Copper plating was used prior to sectioning.

RESULTS AND DISCUSSION

650°C OXIDATION RESULTS

Figure 1 shows typical behavior of coated and uncoated specimens at 650°C in air + 10% water vapor. After an incubation period, uncoated T91(Fe-9wt.%Cr-1Mo) and P92(Fe-9wt.%Cr-2W) specimens
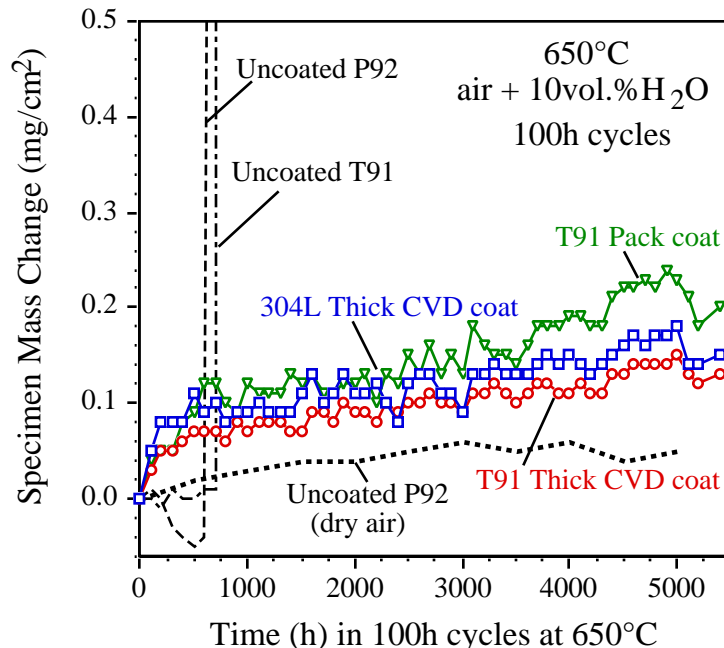
Figure 1. Specimen mass changes during 100h cycles for thick CVD coated 304L and T91 (Fe-9Cr-1Mo) and uncoated T91 and P92 (Fe-9Cr-2W) alloys at 650°C in air + 10% water vapor.

underwent accelerated oxidation with the formation of a thick Fe-rich oxide. In dry air at 650°C, a low mass gain was observed, Figure 1. Specimens with a thick coating made by CVD or pack cementation did not exhibit accelerated attack after >5 kh of exposure. However, minimal interdiffusion is expected at this temperature[16,19] and coating lifetimes can be extensive (>41 kh for slurry coatings in steam[11]).

700°C OXIDATION RESULTS

To accelerate failure due to interdiffusion of Al with the substrate (thereby lowering the surface Al content), exposures also were conducted at 700° and 800°C. (These temperatures exceed any realistic service condition but are necessary to induce coating failure.) Figure 2 shows the mass gain behavior at 700°C. The aluminized coatings showed low mass gains typical of alumina-forming coatings.[17,18] The exception was the thin CVD coating on T91, which exhibited a very high mass gain after ~10 kh and was stopped after 11 kh (110, 100-h cycles). Iron oxide nodules were observed on the specimen surface in SEM plan view. Figure 3 shows EPMA results from a polished cross-section of coated T91 after exposure. Areas of thin Al-rich surface oxide are still evident but Fe-rich oxide nodules penetrate up to ~50μm into the substrate, Figure 3e. The duplex Fe-rich oxide layer with outward (primarily FeO) and inward-growing (Fe and Cr spinel) layers is typical for Fe-base alloys at this temperature in humid air and steam.[17,22,23] The other feature of note was the fine dispersion of AlN particles (Figs 3b and 3f) beneath the original coating layer. These particles are typical in N-containing substrates[10,11,26] and may be detrimental to substrate strength as N was preferentially removed from the substrate.

Residual Al profiles were measured by EPMA in areas where oxide nodules had not formed on the surface, Figure 4. A typical low activity Al profile (dashed line) made by the same process is shown for reference. The starting peak Al content was ~18 at% and was reduced to ~3.5 at% after 11 kh. The maximum Al diffusion depth increased from ~50μm to ~195μm. In each of the three post-exposure profiles, there are peak points in the profile that correspond to the AlN precipitates. Some Al was lost due to oxide formation, but >50% (based on the area under the Al curve) of the Al reduction at the coating surface was due to
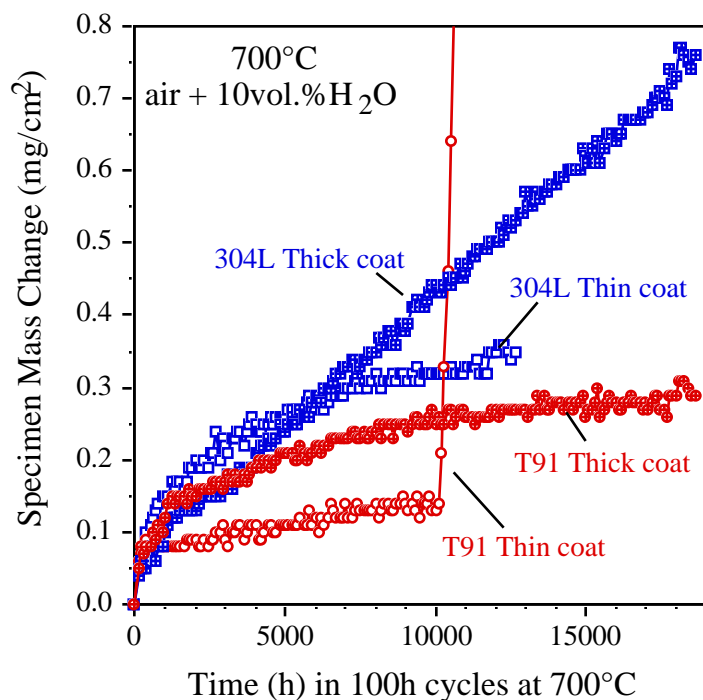
Figure 2. Specimen mass changes during 100h cycles at 700°C in air+10%H$_2$O. Results are shown for uncoated and coated specimens with different coating thicknesses.

interdiffusion with the substrate. (A more accurate analysis will require further characterization of the AlN volume fraction to accurately account for Al in these precipitates.) The apparent C_b value of 3.5at% is significantly lower than the 20%Al needed for sulfidation resistance[17,28,29] but somewhat higher than observed for Fe-13Cr+Al alloys, where only ~2.1at.% Al was needed for resistance to water vapor at
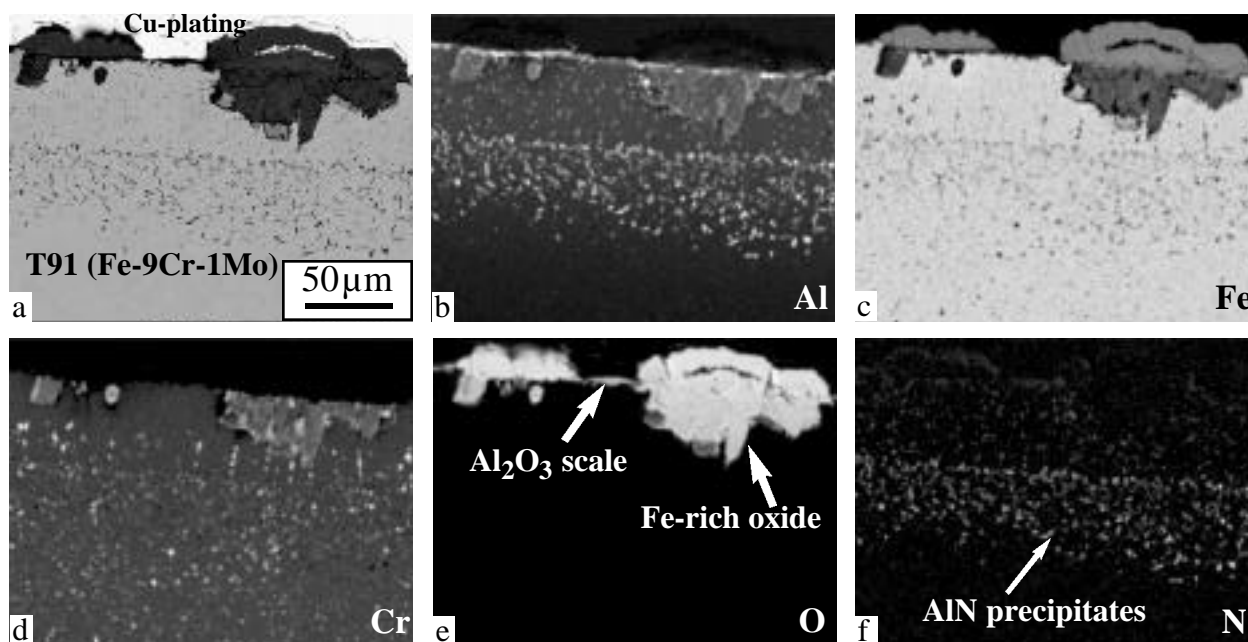
Figure 3. Polished section of CVD thin coating on T91 after 11kh at 700°C in humid air. (a) secondary electron image and EPMA x-ray maps of (b) Al, (c) Fe, (d) Cr, (e) O and (f) N.
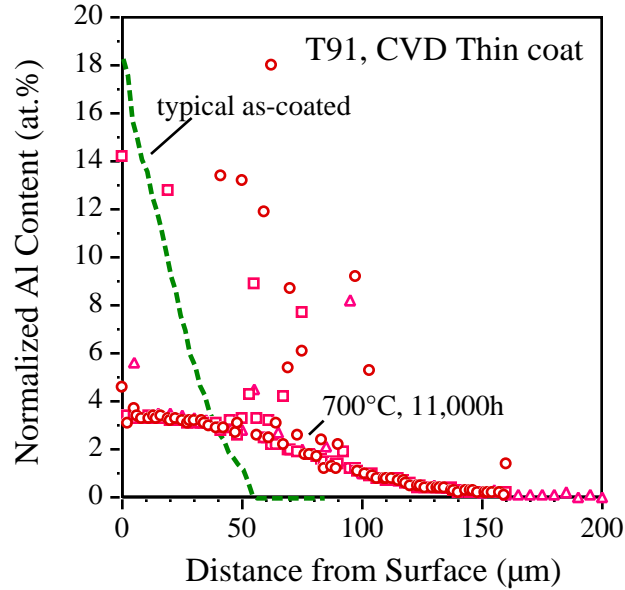
Figure 4. Normalized Al content by EPMA as a function of depth for as-deposited CVD thin coat on T91 (dashed line) and after 11kh at 700°C.

680°C.[23] However, the higher alloy Cr content (13%) would be expected to lower C_b,[22] as would the lower temperature and water vapor content (<2.5%) in the prior work.[23] The effect of Cr content also may explain why the thin coating on 304L has not failed after 12 kh at 700°C, Figure 2. The 304L substrate and coating contain ~19at,%Cr and this should improve the selective oxidation of Al by a third element effect,[27] and likely reduce C_b.

This newly-measured value of C_b can now be entered into the lifetime model[16] to predict oxidation behavior as a function of temperature and starting Al content. Initial calculations indicate that the thick coating would have a lifetime of >550kh at 700°C. Of course, the result also must consider that Al would diffuse to >2mm into the tube wall and compromise the substrate creep strength.[19]
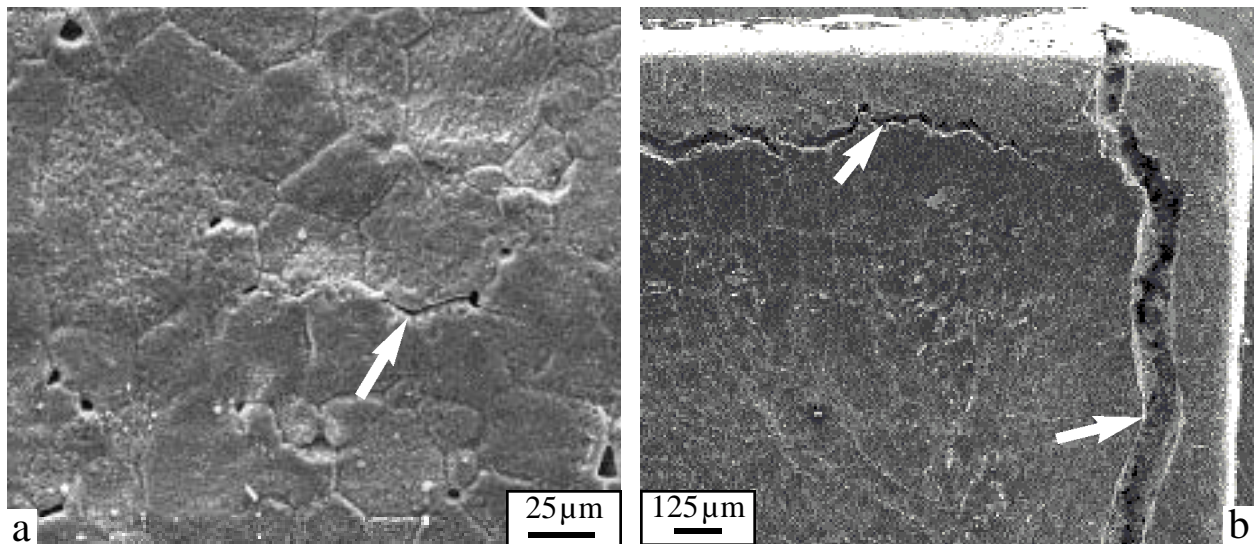

Figure 5. SEM secondary electron plan-view images of coated specimens exposed for 180, 100-h cycles at 700°C in humid air; (a) T91 and (b) 304L. Arrows point to cracks in the coating.

For the thick coatings at 700°C, Figure 2, the T91 substrate showed nearly parabolic behavior after ~19kh. For the 304L substrate, the mass gain was higher than for the thin coating with almost linear kinetics. This difference is attributed to more severe cracking on the specimen face, and particularly the specimen edge, compared to coated T91, Figure 5. The damage at the edge of the coated 304L specimen is similar to that observed during 1h cycles.[18] Thick coated T91 showed no macroscopic cracking at the edges but did show fine cracks in the face, arrow in Figure 5a. One important difference between the two substrates is that on T91 the ~160µm thick interdiffusion zone is also ferritic, so the only CTE mismatch is between the ~40µm Al-rich (Fe_3Al) outer layer and the substrate (~20 and ~13 ppm/K at 700°C, respectively).[17] On 304L, Al interdiffusion resulted in a ferritic layer as well as the intermetallic, $(Fe,Ni)_3Al$ outer layer, resulting in three layers with three different CTEs.[17,18] The increased cracking observed on the coated 304L specimen led to additional oxidation hence the higher rate of mass gain. The lower mass gain for both of the thinner coatings, Figure 2, is likely due to a reduction in the mismatch strain energy with the thinner coating layers, and thus reduced cracking. When the thin coating failed on T91, there was no indication of cracks in the coating, only nodule formation typical of accelerated attack due to the presence of water vapor.

800°C RESULTS

Figure 6 shows mass gains for thick coatings exposed at 800°C. As at 700°C, the coatings on T91 tended to show lower mass gains than those on 304L substrates. The exposure of coated 304L was stopped after 6kh. A similar thick coating on T91 also was exposed for 6kh. This specimen showed a higher mass gain than the nominally similar coated T91 specimen that has been exposed >14kh, Figure 6. (This may be related to scale spallation observed on the latter or excessive oxidation on the former.) Figure 7 shows cross-sections of the coated specimens after 6kh. The coated 304L substrate showed significant deformation compared to the ferritic substrate. As discussed earlier, this was attributed to the CTE mismatch of the thicker ferritic interdiffusion layer with the austenitic substrate. The higher mass gain for the coated 304L specimen was attributed to complete oxidation of the outer layer in some locations, arrows in Figure 7a. An oxide layer formed on the surface and at the interface between the inner and outer layer, Figure 8. In some cases, the outer layer appeared to have been cracked but the cracking did not continue into the inner layer, as after exposure in 1h cycles.[18] Residual Al profiles in the coating are shown in Figure 9a. The outer layer appeared to be a mixture of ~45Ni-37Al-12Fe and ~Fe-14Cr-3Al phases. The
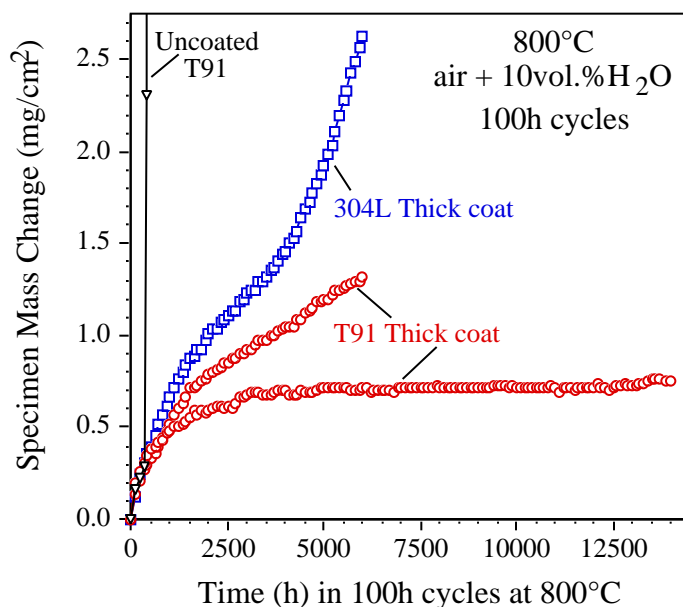

Figure 6. Specimen mass changes during 100h cycles at 800°C in air+10%H_2O.
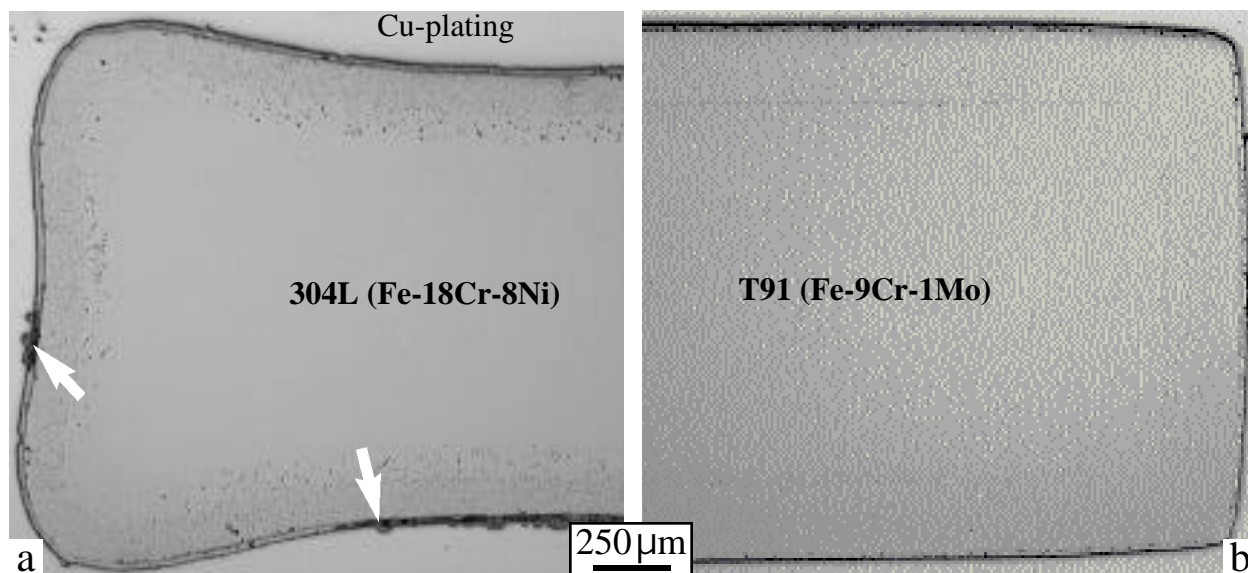
Figure 7. Light microscopy of polished sections of CVD thick coatings after 6kh at 800°C in humid air. (a) 304L substrate and (b) T91 substrate.

NiAl phase is darker gray in Figure 8b. The matrix of the inner layer contained only 4.5%Al (Figure 9a) as well as some Al-rich NiAl particles, Figure 8. The inner layer had increased in depth to ~260µm compared to the starting thickness of ~140µm, Figure 9a. The slower Al diffusivity and Al-induced phase transformation (of the austenitic substrate to ferrite)[3] reduced the starting coating Al content compared to T91 (Figure 9b), limited interdiffusion to some degree and made a more abrupt diffusion profile than in T91, Figures 4 and 9b.

A higher magnification of the coating on T91 after 6kh showed similar degradation of the outer layer, Figure 10. Some oxide had formed at the interface with the inner layer, which may explain the higher mass gain compared to the other coated T91 specimen, Figure 6. Because of the cracks and internal oxidation, the Al profile (Figure 9b) indicated that the outer layer is depleted in Al compared to the inner layer, which still contains ~8% Al. Based on the previous diffusion tests, where the Al content had dropped from 26% to 12% at the surface after 2kh at 800°C, this observation is consistent with the model prediction.[16] The residual Al profile extends to the center of the 1.5mm thick specimen, Figure 9b. Based on these
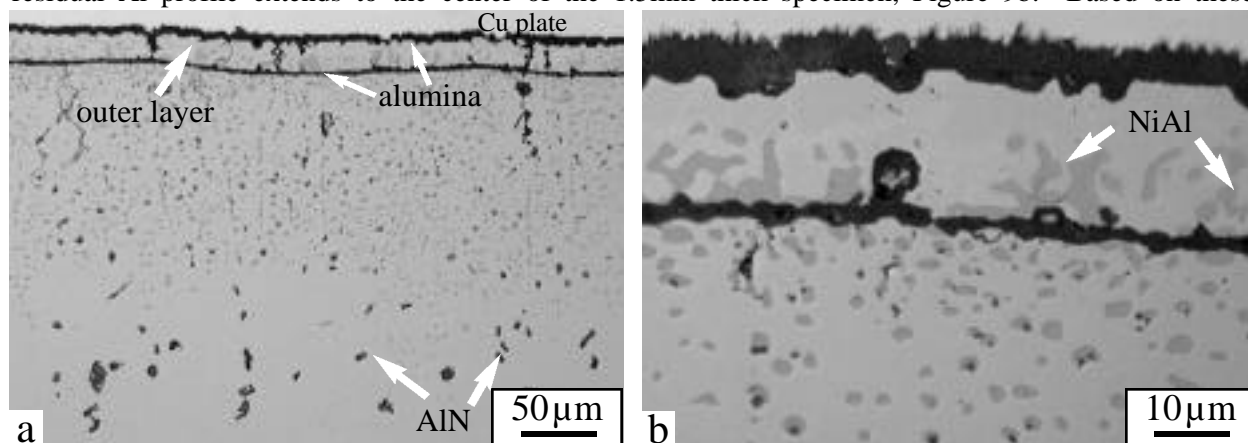

Figure 8. Light microscopy of polished section of CVD thick coating on 304Lsubstrate after 6kh at 800°C in humid air; oxide formed at the interface between the inner (ferritic, low Al) and outer (intermetallic, high Al) coating layers. (b) The darker gray phase in the coating is -NiAl.
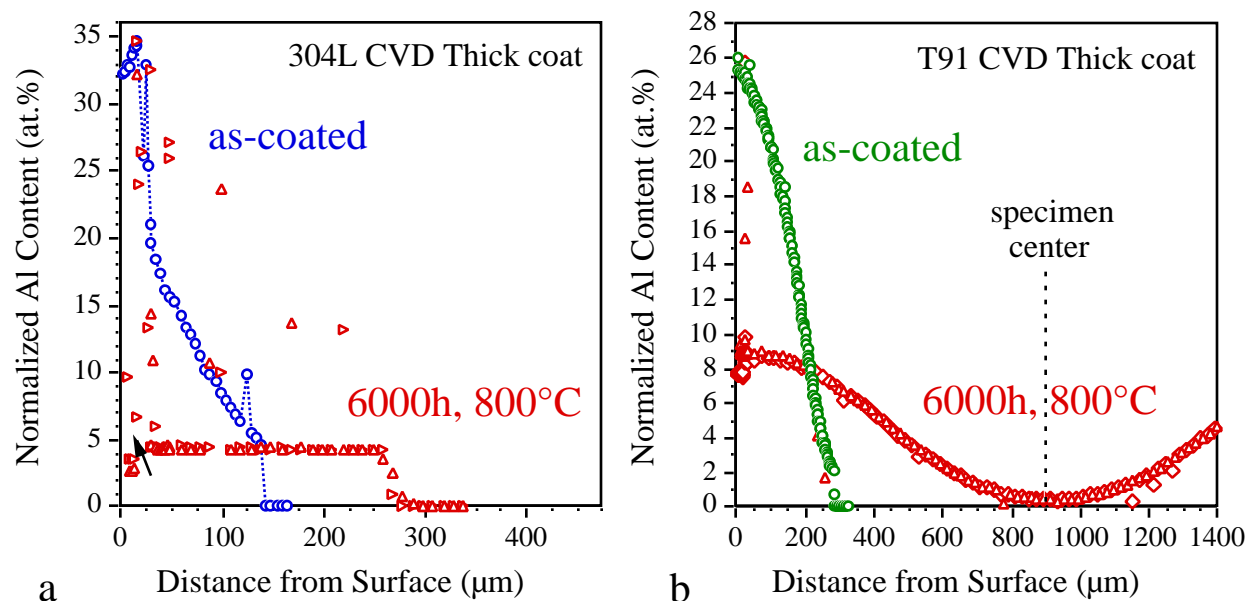
Figure 9. Normalized Al content by EPMA as a function of depth for CVD thick coatings on (a) 304L and (b) T91, as-coated and after 6 kh at 800°C.

observations, it is unlikely that the other coated T91 specimen will experience accelerated oxidation (i.e. coating Al content below C_b) in the near future, although the outer layer may experience breakaway oxidation similar to the 304L specimen.

650°C Creep Testing

Figures 11 and 12 summarize the steady-state creep rates from P92 specimens cut from a pipe with various coatings and heat treatments. Some coating studies have maintained the coating temperature at 700°C in order to avoid disrupting the ferritic-martensitic (FM) microstructure.[10,11] However, these coatings tend to form high-Al, brittle phases such as Fe_2Al_5. Steels like P92 are typically given a two stage heat treatment of austenization for ~1 h at 1050°C (designated HT) followed by quenching in air and then tempering for ~2 h at 750°C (designated LT). The creep rates for uncoated P92 in Figure 11a show that an HT heat treatment followed by slow cooling, similar to a pack or CVD coating process, did not adversely affect the creep rate compared to as-received, fully heat-treated P92. However, the HT exposure did
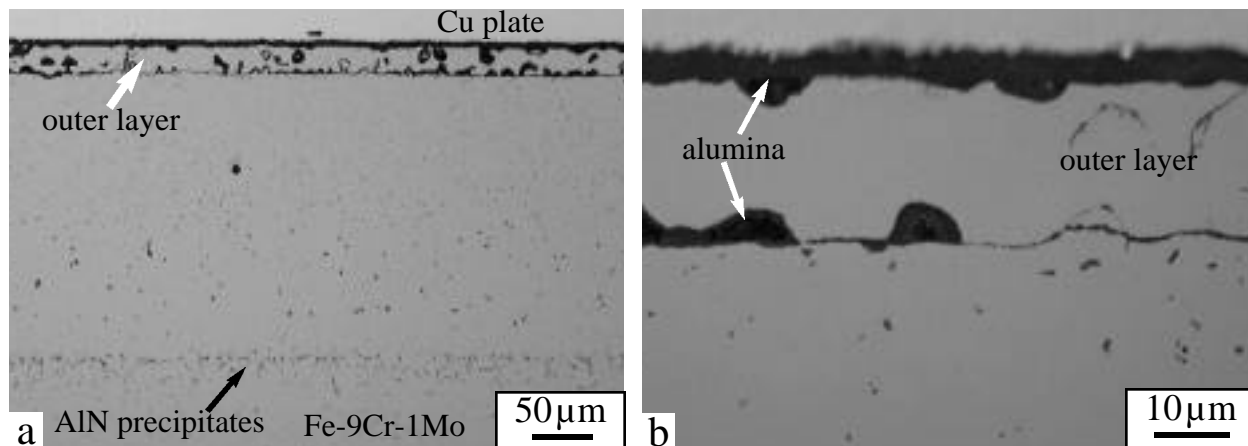

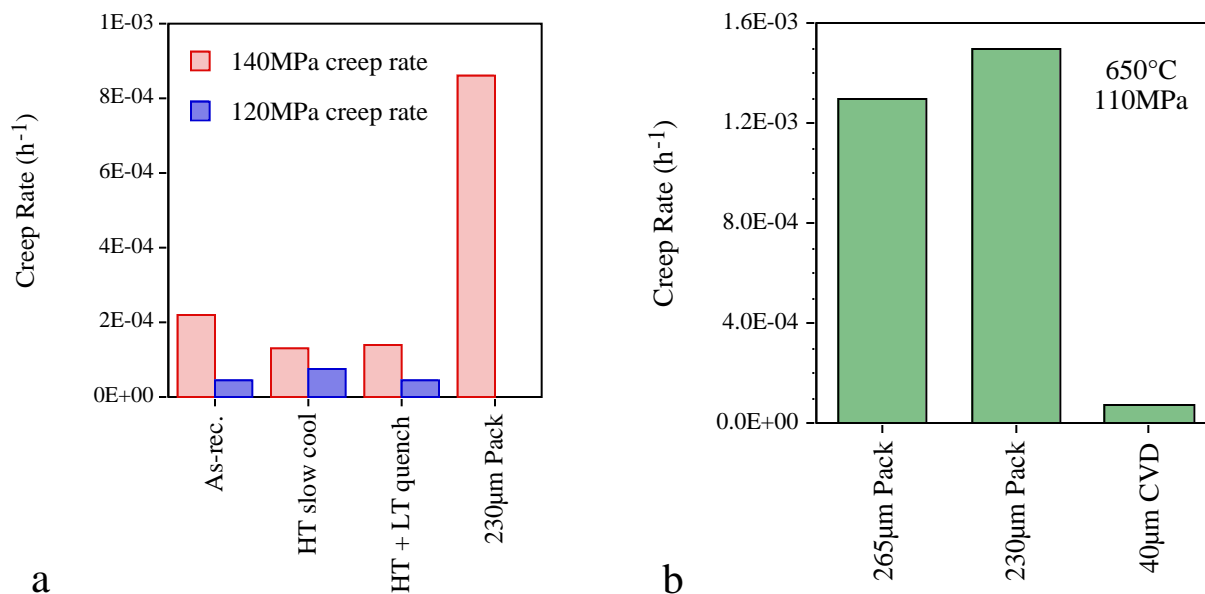Figure 10. Light microscopy of polished section of CVD thick coating on T91 after 6 kh at 800°C in humid air.

Figure 11. Steady-state creep rates for P92 specimens with and without aluminide coatings and various heat treatments (HT: 1h, 1050°C; LT: 2h,750°C) tested at 110-140 MPa at 650°C in laboratory air.

coarsen the microstructure which may reduce the fracture toughness. A P92 specimen given a HT anneal and subsequent LT anneal followed by quenching also showed a similar creep rate, Figure 11a.

The effect of aluminizing also is shown in Figure 11. A typical ~230µm thick pack coating had a significant negative effect on the creep rate. The effect could be modeled by assuming that the coated area of the gage had no creep strength and only the unaffected substrate supported the applied load.[19] With only a 2x2mm gage, a second series of thin pack and CVD coatings were made for testing with significantly lower creep rates compared to the thicker coatings, Figure 11b and 12. A combination of alternating creep (~200h) and corrosion (5, 100-h cycles at 650°C in wet air) exposures also were
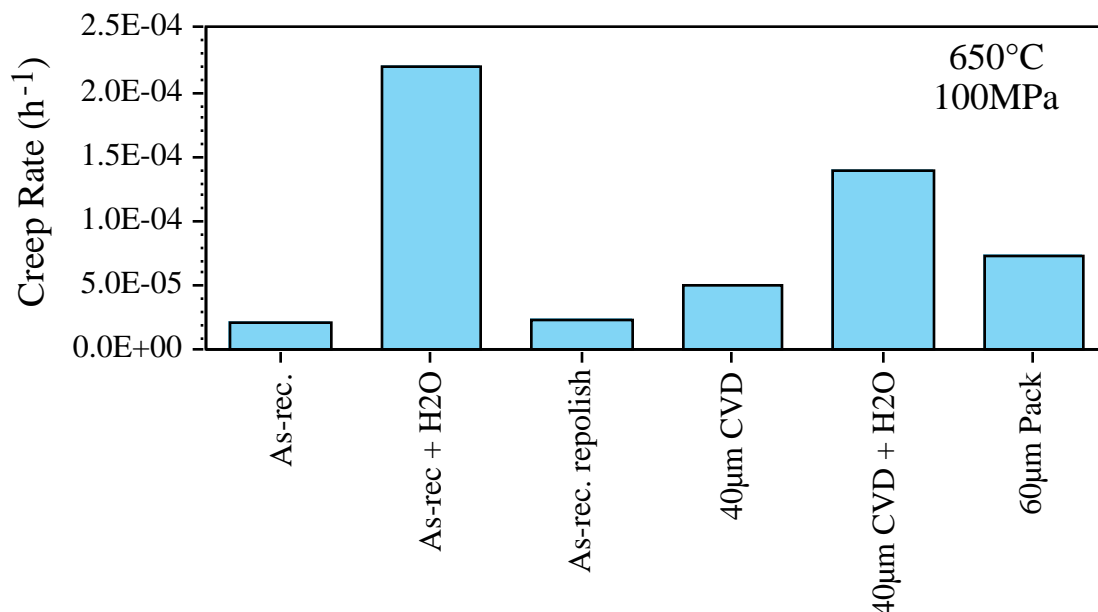

Figure 12. Steady-state creep rates for P92 specimens with and without aluminide coatings tested at 100 MPa at 650°C in laboratory air. Some specimens were tested after exposure for 500h at 650°C in wet air (+ H$_2$O).

performed.[30] The goal of this work was to quantify the effect on the creep rate of a thick Fe-rich oxide forming on uncoated P92 and consuming substrate. However, a significant difference was noted between specimens that were first creep tested and then exposed to water vapor and specimens that were exposed to water vapor first (+H_2O in Figure 12). The prior exposure in water vapor increased the creep rate of both coated and uncoated specimens. Also, the creep rate of the uncoated specimens did not increase during further corrosion exposures in wet air when the oxide continued to grow and consume the gage section. The unexpected results suggested that the thick oxide layer may be load bearing. In order to avoid these complications, future creep testing should be conducted in wet air or steam environments to observe the effect of environment on mechanical properties.

SUMMARY

Long-term oxidation performance of coated ferritic (T91) and Fe-base austenitic (304L) substrates were conducted in humid air at 650°-800°C. The higher temperatures were used to accelerate the Al interdiffusion to create coating failures. Using 100h exposure cycles, none of the thicker coatings showed accelerated attack of the substrate at the higher temperatures. A thinner coating on T91 failed after ~10,000h at 700°C, allowing rapid oxidation of the substrate when only ~3.5at.%Al remained in the coating. This result established a minimum Al content for modeling coating lifetime. In general, aluminide coatings on 304L substrates showed higher mass gains and more degradation than similar coatings on T91 substrates. This difference is attributed to the Al-induced phase transformation from austenite to ferrite in the interdiffusion zone, causing more severe CTE mismatch problems. Creep testing of coated and uncoated P92 specimens was conducted at 650°C to evaluate the effect of heat treatments and coating on the substrate steady-state creep properties.

ACKNOWLEDGMENTS

REFERENCES

1.   N. R. Lindblad, *Oxid. Met.*, 1 (1969) 143.
2.   J. L. Smialek and C. E. Lowell, *J. Electrochem. Soc.*, 121 (1974) 800.
3.   N. V. Bangaru and R. C. Krutenat, *J. Vac. Sci. Tech. B*, 2 (1984) 806.
4.   G. W. Goward, *Mater. Sci. Tech.*, 2 (1986) 194.
5.   D. M. Miller, S. C. Kung, S. D. Scarberry and R. A. Rapp, *Oxid. Met.*, 29 (1988) 239.
6.   B. M. Warnes and D.C. Punola, *Surf. Coat. Tech.*, 94-95 (1997) 1.
7.   M. Zheng and R. A. Rapp, *Oxid. Met.*, 49 (1998) 19.
8.   B. A. Pint, I. G. Wright, W. Y. Lee, Y. Zhang, K. Prüßner and K. B. Alexander, *Mater. Sci. Eng.*, A245 (1998) 201.
9.   K. Bouhanek, O. A. Adesanya, F. H. Stott, P. Skeldon, D. G. Lees and G. C. Wood, *Mater. Sci. Forum*, 369-372 (2001) 615.
10.   V. Rohr and M. Schütze, *Mater. Sci. Forum*, 461-464 (2004) 401.
11.   A. Agüero, R. Muelas, M. Gutiérrez, R. Van Vulpen, S. Osgerby and J. P. Banks, *Surf. Coat. Tech.*,

201 (2007) 6253.

12. V. Deodeshmukh, N. Mu, B. Li and B. Gleeson, *Surf. Coat.Tech.*, 201 (2006) 2836
13. E. J. Opila, *Mater. Sci. Forum*, 461-464 (2004) 765
14. R. Viswanathan and W. Bakker, *J. Mater. Eng. Performance*, 10 (1) (2001) 81
15 S. W. Banovic, J. N. Du Pont and A. R. Marder, *Mater. High Temp.*, 16 (1999) 195
16. Y. Zhang, A. P. Liu and B. A. Pint, *Mater. Corr.*, in press (2007)
17. B. A. Pint, Y. Zhang, P. F. Tortorelli, J. A. Haynes and I. G. Wright, *Mater. High Temp.*, 18 (2001) 185
18. Y. Zhang, B. A. Pint, G. W. Garner, K. M. Cooley and J. A. Haynes, *Surf. Coat. Tech*., 188-189 (2004) 35
19. S. Dryepondt, Y. Zhang and B. A. Pint, *Surf. Coat.Tech.*, 201 (2006) 3880
20. W. Y. Lee, Y. Zhang, I. G. Wright, B. A. Pint and P. K. Liaw, *Met. Trans.*, 29A (1998) 833
21. B. A. Pint, R. Peraldi and P. J. Maziasz, *Mater. Sci. Forum*, 461-464 (2004) 815
22. B. A. Pint and I. G. Wright, *Mater. Sci. Forum*, 461-464 (2004) 799
23. I. Kvernes, M. Olivera and P. Kofstad, *Corr. Sci.*, 17 (1977) 237
24. Y. Zhang, B. A. Pint, K. M. Cooley and J. A. Haynes, in preparation
25. Y. Zhang, Y. Q. Wang and B. A. Pint, NACE Paper 07-468, Houston, TX, presented at NACE Corrosion 2007, Nashville, TN, March 2007
26. Y. Zhang, B. A. Pint, K. M. Cooley and J. A. Haynes, *Surf. Coat.Tech.*, 200 (2005) 1231
27. F. H. Stott, G. C. Wood and J. Stringer, *Oxid. Met.*, 44 (1995) 113.
28. P. F. Tortorelli and J. H. DeVan, *Mat. Sci. and Eng.*, A153 (1992) 573.
29. P. F. Tortorelli and K. Natesan, *Mater. Sci. Eng.*, A258 (1998) 115.
30. S. Dryepondt, Y. Zhang and B. A. Pint, NACE Paper 07-471, Houston, TX, presented at NACE Corrosion 2007, Nashville, TN, March 2007